Modeling Time-Dependent Corrosion Fatigue Crack Propagation in 7000 Series Aluminum Alloys

Mark E. Mason and Richard P. Gangloff

Center for Electrochemical Science and Engineering
Department of Materials Science and Engineering
University of Virginia
Charlottesville, VA 22903

ABSTRACT

Stress corrosion cracking and corrosion fatigue experiments were conducted with the susceptible S-L orientation of AA7075-T651, immersed in acidified and inhibited NaCl solution, to provide a basis for incorporating environmental effects into fatigue crack propagation life prediction codes such as NASA FLAGRO. This environment enhances da/dN by five to ten-fold compared to fatigue in moist air. Time-based crack growth rates from quasi-static load experiments are an order of magnitude too small for accurate linear superposition prediction of da/dN for loading frequencies above 0.001 Hz. Alternate methods of establishing da/dt, based on rising-load or ripple-load-enhanced crack tip strain rate, do not increase da/dt and do not improve linear superposition. Corrosion fatigue is characterized by two regimes of frequency dependence; da/dN is proportional to f^{-1} below 0.001 Hz and to f^{0} to $f^{-0.1}$ for higher frequencies. Da/dN increases mildly with both increasing hold-time at K_{MAX} and with increasing rise-time for a range of loading waveforms. The mild time-dependence is due to cycle-time-dependent corrosion fatigue growth. This behavior is identical for S-L and L-T crack orientations. The frequency response of environmental fatigue in several 7000 series alloys is variable and depends on undefined compositional or microstructural variables. Speculative explanations are based on the effect of Mg on occluded crack chemistry and embrittling hydrogen uptake, or on variable hydrogen diffusion in the crack tip process zone. Cracking in the 7075/NaCl system is adequately described for life prediction by linear superposition for prolonged load-cycle periods, and by a time-independent upper bound relationship between da/dN and ΔK for moderate loading times.

INTRODUCTION

A variety of chemical and electrochemical environments enhance rates of fatigue crack propagation (FCP) in aluminum and titanium alloys,[1,2] however, such behavior is not described sufficiently in fracture mechanics-based life prediction codes such as NASA FLAGRO.[3,4] Two issues are particularly important: the complex dependence of environmental fatigue crack propagation (EFCP) rate (da/dN) on stress intensity range (ΔK) and stress ratio (R), including both intrinsic damage and crack closure contributions, as well as the time and crack tip strain rate dependencies of

da/dN. This paper considers the latter issue for aqueous chloride EFCP in precipitation hardened 7000-series aluminum alloys.

Work to date demonstrated that loading frequency (f),[5-11] waveform[9,10,12,13] and hold-time (τ_H)[9,10,13] affect EFCP rates for aluminum alloys such as 7075-T6 in full immersion chloride solutions at 25°C. Da/dN vs f data are summarized in Fig. 1, and demonstrate this strong and time-dependent environmental effect for several alloys.[5-7,11] [1] While da/dN is always frequency-independent for FCP in either vacuum or moist air at frequencies below 50 Hz, three frequency dependencies are observed for the chloride cases. So-called true corrosion fatigue involves frequency-independent cracking at rates well above the benign environment values, as shown approximately for 7075 at frequencies above about 10^{-3} Hz.[1,5] Purely time-dependent FCP is indicated by da/dN data that are proportional to 1/f for 7079 and 7075 at frequencies below 1 and 10^{-3} Hz, respectively.[5,11] Cycle-time dependent corrosion fatigue is characterized by $da/dN \propto f^{-\beta}$, where ß is on the order of 1/2, as observed for 7017 and 7475.[6,7] The underlying causes for the varied EFCP resistances and frequency dependencies shown for similar 7000 alloys in Fig. 1 are not understood.

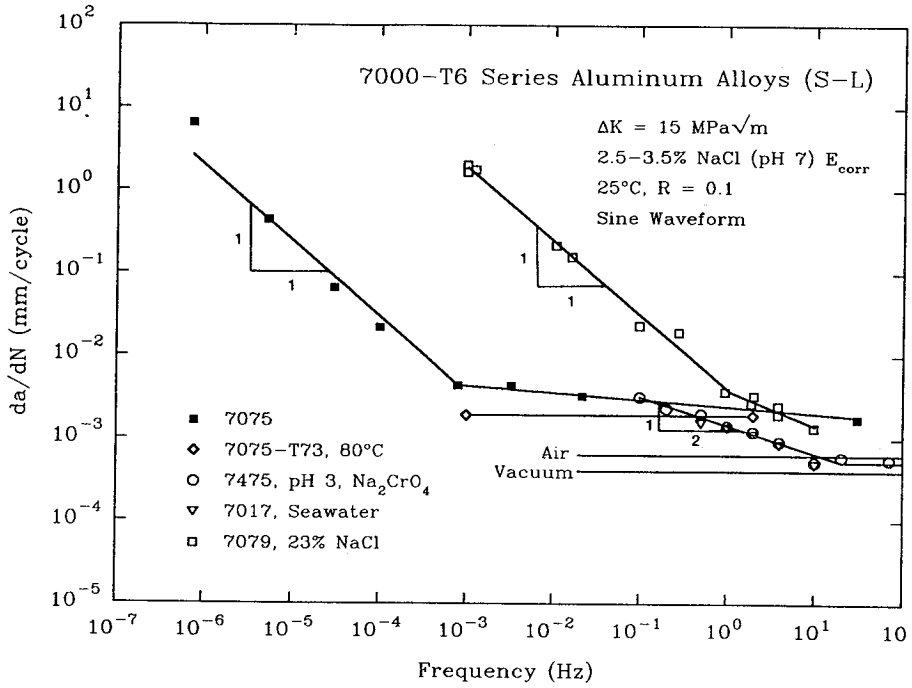

Figure 1 - Effect of frequency on corrosion fatigue crack propagation in 7000 series aluminum alloys in aqueous chloride.[5-7,11]

The EFCP frequency dependencies shown in Fig. 1 can be modeled based on empirical curve-fitting[14], linear superposition[15], or mass transport and chemical reaction kinetics.[1,16] The simple linear superposition approach may be applicable to EFCP in 7000-series aluminum alloys because of the low threshold stress intensity (K_{ISCC} or K_{TH}) of about 5 MPa√m for such alloys, particularly in the S-L orientation.[5,17] This method equates the total environmental da/dN to the sum of the crack growth rate per load cycle due to fatigue damage in an inert environment (da/dN_{Mech}) and the contribution from time and K-dependent monotonic-load environmental cracking ($da/dt_{SCC}(K)$), integrated over a portion of each fatigue cycle (τ) where K(t) exceeds K_{ISCC}:

---

1 The data in Fig. 1 were obtained for constant applied ΔK, R, a sinusoidal loading waveform, and S-L crack orientation (loading is parallel to the plate thickness (S) direction and the crack growth direction is parallel to the rolling (longitudinal-L) direction). Modest variations from the constant solution chemistry of 2.5 to 3.5 wt% NaCl, pH 7, aerated free corrosion potential, and 25°C are noted. All data were obtained for an applied ΔK of 15 MPa√m with the exception of the results for 7075-T6[11]. These data were measured for a single ΔK of 9.5 MPa√m (R=0.3) and extrapolated to 15 MPa√m (R=0.1) by the Forman crack growth rate relationship.[3]

$$\frac{da}{dN} = \frac{da}{dN_{Mech}} + \int_{\tau} \left[\frac{da}{dt_{SCC}}(K)\right] K(t)\,dt \qquad (1)$$

τ often defines the loading-only portion of the fatigue cycle where process zone stresses are tensile. Traditionally, da/dt_{SCC} has been determined by either constant load or constant crack mouth opening displacement experiments, and is K-independent for aluminum alloys in chloride above K_{ISCC}.[17] For this case, and when da/dN_{Mech} is a small fraction of da/dN, Eq. 1 leads to the prediction that da/dN depends on 1/f, as observed for 7079 in NaCl (at frequencies less than 1 Hz) and for 7075 (at $f < 0.001$ Hz, Fig. 1). For these two cases, linear superposition effectively predicts the effects of ΔK, R, f, hold time, and wave form on environmental da/dN.

Holroyd and Hardie demonstrated that linear superposition was incapable of describing the magnitude of da/dN and the frequency dependence of FCP for 7017 in seawater (Fig. 1).[6] Although K_{ISCC} was low, da/dt_{SCC} from quasi-static load testing was too small to account for the necessary time-dependent enhancement over da/dN_{Mech} through Eq. 1. For this case, the time-dependence is considered based on:

$$\frac{da}{dN} = \frac{da}{dt}\,\frac{1}{\alpha f} \qquad (2)$$

where da/dt is the average time-based crack growth rate during a fraction ($1/\alpha$) of the load cycle and may be frequency-dependent. If da/dt increases with increasing frequency, raised to a power (n) on the order of one-half[18], then da/dN will vary with $f^{(n-1)}$ or $f^{-\beta}$, as indicated in Fig. 1. The implication of this argument is that da/dt should be measured for crack tip strain rates typical of FCP; quasi-static load experiments may not yield relevant time-based crack growth rates for modeling EFCP da/dN. For example, da/dt could be determined from EFCP experiments conducted with several hold times and analyzed with Eq. 1.[13] Alternately, da/dt could be measured by a rising load or rising displacement method that systematically varies crack tip strain rate and stress intensity;[19] the issue is whether such growth rates exceed da/dt_{SCC} determined from quasi-static load or displacement experiments. Strain rate-dependent da/dt is understandable from the film rupture and transient dissolution/ repassivation perspective.[18] Both this mechanism and hydrogen environment embrittlement must be considered to predict time-cycle-dependent EFCP.[1,16,18]

OBJECTIVE AND APPROACH

The objectives of this research on an SCC-susceptible 7000-series aluminum alloy in aqueous chloride are four-fold: (1) to test static load or displacement-based linear superposition predictions of da/dN vs ΔK and f, (2) to determine if da/dt_{SCC} is affected sufficiently by crack tip strain rate to enable improved linear superposition predictions of da/dN, (3) to measure the frequency, load waveform and hold-time dependencies of da/dN, and (4) to speculate on the metallurgical and electrochemical origin(s) of the important variability shown in Fig. 1. The output of this work will be improved data and understanding on time-cycle-dependent EFCP kinetics for use in NASA-FLAGRO.

Constant load/displacement, monotonically rising load, and ripple load experiments are conducted with a cracked fracture mechanics specimen to determine the stress intensity and crack tip strain rate dependencies of da/dt_{SCC}. Computer-automated constant ΔK and ΔK-decreasing experiments are employed to determine da/dN as a function of loading frequency, waveform and hold-time.

EXPERIMENTAL PROCEDURE

Material

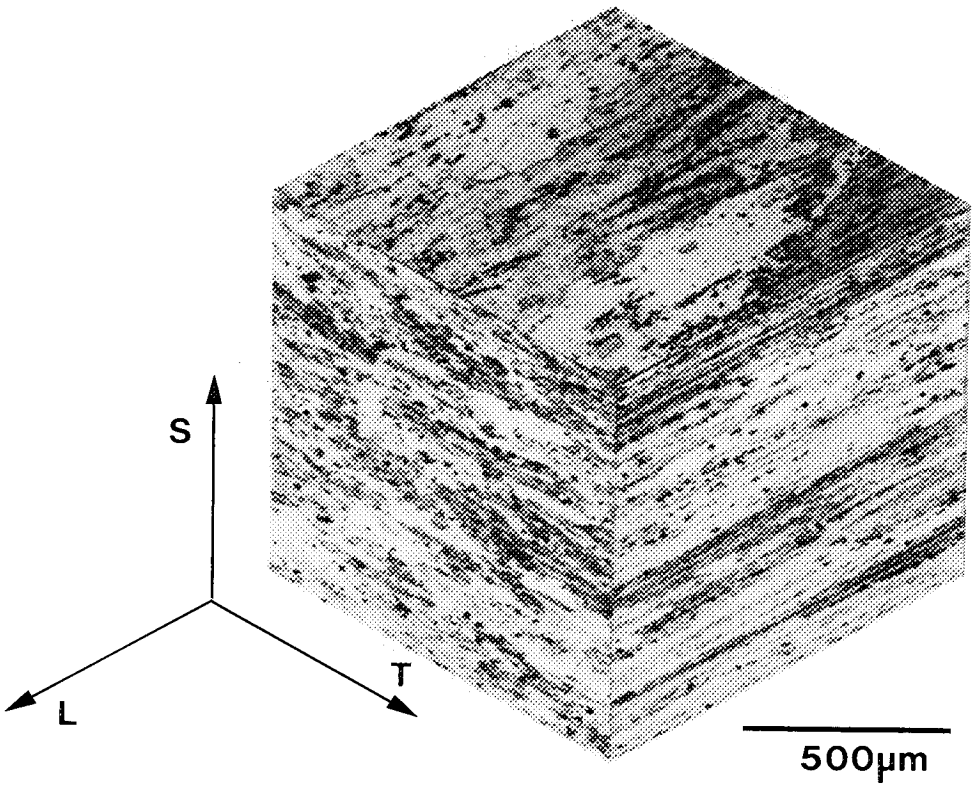

Al-Zn-Mg-Cu alloy 7075 (52 mm-thick rolled plate) was studied in the peak-aged, T651 condition (24 hrs at 120 to 124°C). Chemical composition and mechanical properties are given in Table I. The optical micrographs shown in Fig. 2 reveal large flattened grains elongated in the rolling direction. Average grain dimensions in the L, transverse (T), and S directions are 1 mm, 200 μm, and 10 to 20 μm, respectively. This lot of material was previously studied in an ASTM interlaboratory test program on stress corrosion cracking.[20]

Figure 2 - Representative microstructure of 7075-T651 aluminum alloy. Magnification 52X.

Table I. Nominal Chemical Composition and Mechanical Properties of 7075-T651

Chemical Composition (wt pct)

Zn	Mg	Cu	Cr	Mn	Ti	Fe	Si	Al
5.1-6.1	2.1-2.9	1.2-2.0	0.18-0.4	0.3 max	0.2 max	0.7 max	0.5 max	bal.

Mechanical Properties

Yield Strength MPa (ksi) *	Tensile Strength MPa (ksi) *	Elongation Pct *	K_{IC}, MPa$\sqrt{m}$ (ksi$\sqrt{in}$) **
472 (68.4)	540 (78.2)	4.0	22.2 (19.3)

* Loading axis parallel to L.
** S-L orientation.

Crack Growth Measurement

The wedge-opening-load (WOL) specimen (thickness, B = 7.6 mm; width, W = 52.3 mm; and half-height to width ratio, H/W = 0.486), machined from the plate in the S-L orientation was used throughout. Specimens were mounted in the load train via clevises with roller bearings at the load pins to provide free rotation. Established stress intensity and compliance solutions were utilized for the WOL specimen.[21] Experiments were performed using a closed-loop servo-hydraulic test machine interfaced to a personal computer for automated stress intensity control during both monotonic and fatigue loading. Crack mouth opening displacement (CMOD), load, and crack length from direct current electrical potential (DCPD) were continuously measured and variously used as the active control signal. The DCPD solution for the compact tension specimen was successfully employed for the similar WOL geometry.[22,23]

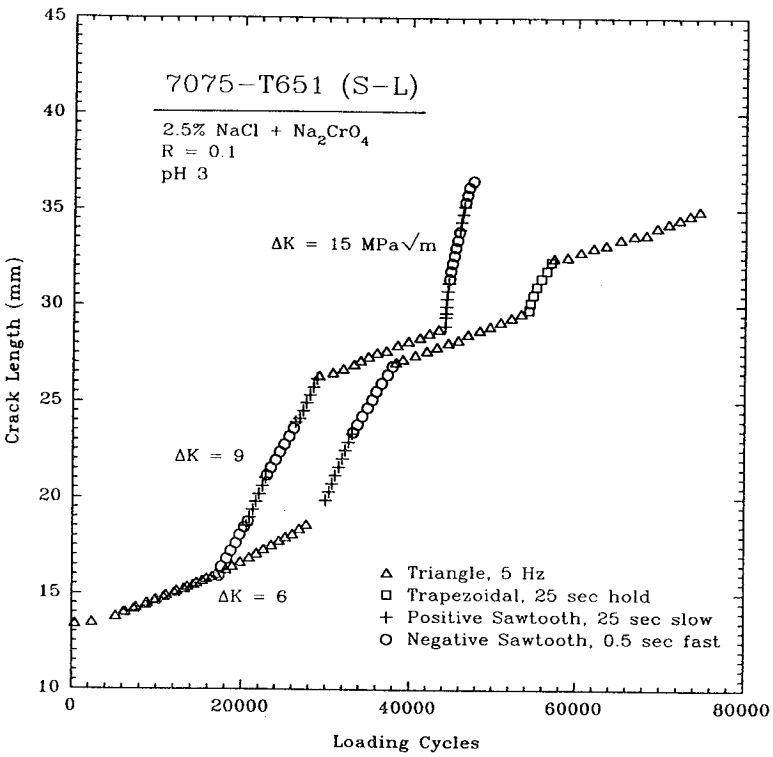

Figure 3 - Fatigue crack length *vs* loading cycles at constant ΔK (6, 9, 15 MPa$\sqrt{m}$; R=0.1) for peak-aged 7075 (S-L orientation) in NaCl.

CMOD, measured by an extensometer, controlled the rising load and constant displacement experiments; additional experiments were conducted at constant load. Crack length was measured by DCPD for each case. Both constant ΔK and ΔK-decreasing experiments were conducted in load control, were based on DCPD crack lengths, and followed standardized procedures.[22] The machine control software provided a variety of cyclic loading frequencies, hold-times and waveforms. Fig. 3 shows cyclic crack length data from two typical constant stress intensity range EFCP experiments aimed at determining da/dN (from linear regression of crack length, a, vs loading cycles, N) for positive and negative

sawtooth, trapezoidal and triangular waveforms at three constant ΔK levels. This procedure provides steady-state EFCP growth rates at fixed ΔK and R, distinguishes small differences in da/dN, and provides a qualitative indication of the effect of crack closure (which could change with increasing crack length and specimen immersion time). Changing loading conditions often marked the fracture surface for post-test visual observations to improve DCPD crack length accuracy by linear error correction.[23] Such measurements verified less than a 10% difference between crack lengths from DCPD and actual values. Corrected crack lengths were employed for all calculations of da/dN and ΔK. Fatigue crack closure stress intensities were not measured.

Environment

The polymethyl methacrylate (PMMA) environmental cell shown in Fig. 4 was used to fully immerse the crack tip in an aerated solution of deionized water, 2.5 wt pct NaCl, 0.5 wt pct Na_2CrO_4, and dropwise added HCl to decrease the bulk solution pH to 3. Chromate inhibitor, added to facilitate electron microscopy of fracture surfaces, reduces passive current density slightly (0.1 to 0.02 A/m^2) with a negligible decrease in da/dt.[11] Solution was circulated continuously at 1 ml/sec, through the cell and specimen notch parallel to the crack front from a 1 liter reservoir. All experiments were conducted at the open circuit condition, without galvanic coupling of the grounded WOL specimen and test machine. Throughout each experiment, a chloridized silver reference electrode, located within the notch at the specimen midplane, monitored electrode potential which varied by less than ± 50 mV about 770 mV_{SCE}.

RESULTS AND ANALYSIS

Monotonic Load Environmental Cracking

Stress Corrosion Cracking

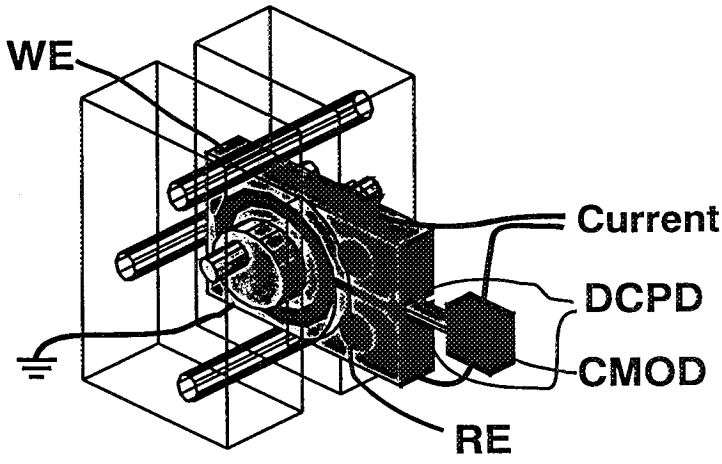

Figure 4 - Schematic of environmental cell and mechanical testing set-up.

The quasi-static load/displacement stress corrosion cracking behavior of 7075, in the susceptible S-L orientation and T651 temper, is summarized by the literature results in Fig. 5.[5,24-26] For full immersion (FI) in neutral NaCl at free corrosion electrode potentials, SCC is characterized by K-independent cracking at a rate of about 10^{-8} m/sec, transitioning to a threshold K_{ISCC} below 4 to 5 MPa$\sqrt{m}$. Extensive, long-term results from multiple-laboratory testing of 7075-T651 (S-L) in 3.5 wt pct NaCl (FI) compare favorably with the data in Fig. 5.[27]

Given these extensive data, only limited experiments were conducted for the heat of 7075-

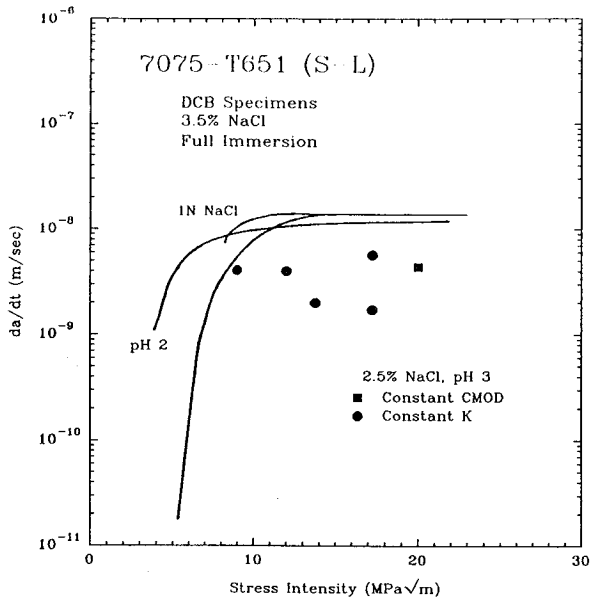

Figure 5 - Effect of stress intensity on da/dt showing K-independent da/dt_{II} above K_{ISCC} for 7075 in chloride.[5,24-26]

T651 (S-L) used in the current study. Measured values of da/dt_{SCC} are plotted as points (● for constant stress intensity and ■ for constant CMOD) in Fig. 5 with constant K applied utilizing DCPD crack length and load as the active feedback. Growth rates averaged over at least 2 mm of crack extension are consistent with K-independent cracking; however, measured da/dt_{SCC} values vary from 2.0 to 4.4 x 10^{-9} m/sec and are slower than the literature results.

Colvin et al. reported an approximate da/dt_{SCC} of 5 x 10^{-9} m/sec based on alternate immersion (AI) exposure of this same heat of 7075 in the T651 temper and for constant displacement.[20] Rechberger reported that da/dt_{SCC} equaled 2 x 10^{-9} m/sec at a K of 10 MPa√m and increased to 1.5 x 10^{-8} m/sec at 18 MPa√m for 7075-T651 (S-L) in neutral NaCl (FI) and at constant load; SCC was not K-independent.[11]

Linear Superposition

For linear superposition modeling, $da/dt_{SCC}(K)$ was equated to the highest measured Stage II velocity of 4.4 x 10^{-9} m/sec for 7075-T651 (S-L), and assuming no crack growth below a K_{ISCC} of 5 MPa√m. FCP rates for L-T 7075-T651 in helium or vacuum comprised the mechanical component.[28] Equation 1 was integrated numerically to yield the predicted EFCP rates that are shown in Fig. 6 for fixed frequencies between 0.01 and 20 Hz, with K varying sinusoidally as a function of time.[29] These predictions are compared with corrosion fatigue data generated with sinusoidal loading at 5 Hz.

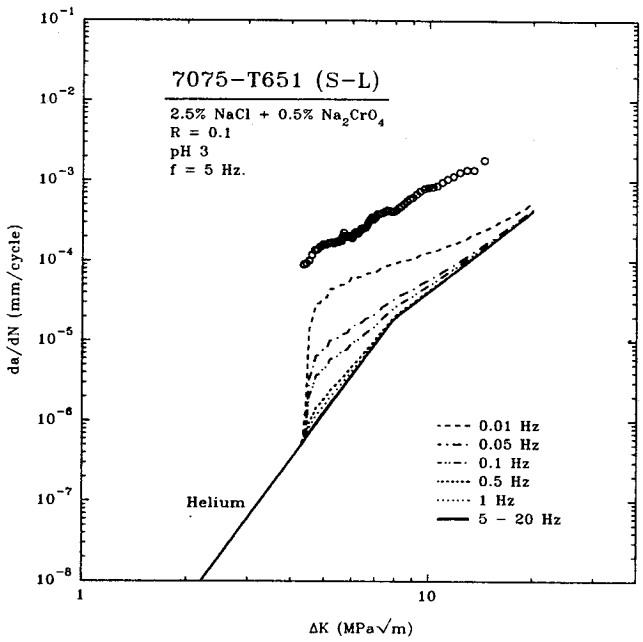

Figure 6 - Linear superposition model predictions of EFCP for the S-L 7075-T651/NaCl (FI) system compared with measured da/dN vs ΔK at f=5 Hz and R=0.1.

Linear superposition underpredicts substantially the 5 Hz EFCP rate for 7075-T651 in NaCl, as reported for 7017 and 7475.[6,7] This error is attributed to the slow da/dt_{SCC} compared to the order of magnitude increase in actual aqueous da/dN values over inert helium. Due to the low value of da/dN_{SCC} relative to da/dN_{Mech}, predicted EFCP rates do not show an inverse frequency dependence for the range above 0.01 Hz.

At ΔK of 15 MPa√m, the measured EFCP rate is 2 x 10^{-3} mm/cycle. Applying Eq. 2 and a

frequency independent da/dt_{SCC} of 4 x 10^{-6} mm/sec, da/dN_{SCC} becomes a dominant factor below frequencies of 0.001 Hz. Fig. 1 confirms that da/dN depends on f^{-1} for 7075, but only for frequencies less than 0.001 Hz.[2]

Crack Tip Strain Rate Effects

The crack tip strain rate ($d\epsilon_{CT}/dt$) during constant load or displacement measurements of K_{ISCC} and da/dt is low for 7075/NaCl due to low levels of the three factors that control $d\epsilon_{CT}/dt$: crack tip creep deformation, dK/dt and da/dt[1,18]. Strain rate, and perhaps da/dt, are increased if the precracked specimen is subjected to a monotonically increasing K at a fixed CMOD rate.

No such effect was detected for 7075-T651 (S-L) in chloride, loaded at a fixed CMOD rate of 2 x 10^{-5} mm/sec. The results in Fig. 7, plotted as the K level where crack extension was first easily detected by DCPD (K_{TH}) versus CMOD rate, show that K_{TH} equals K_{IC} (□) for mechanical failure in moist air. This single result agrees with extensive data from similar rising-load SCC experiments with 2024-T351 (S-L) in NaCl (FI) plotted as the line in Fig. 7.[19] K_{ISCC} for this system equaled 5 to 7 MPa√m and the quasi-static da/dt_{SCC} was 6 x 10^{-9} m/sec. A sharp transition, from K_{TH} equalling K_{ISCC} at low loading rates to K_{TH} equalling K_{IC} at faster rates, was observed at the applied load-line displacement rate of 3 x 10^{-7} mm/sec. (Load-line displacement and CMOD rates are proportional and similar.)

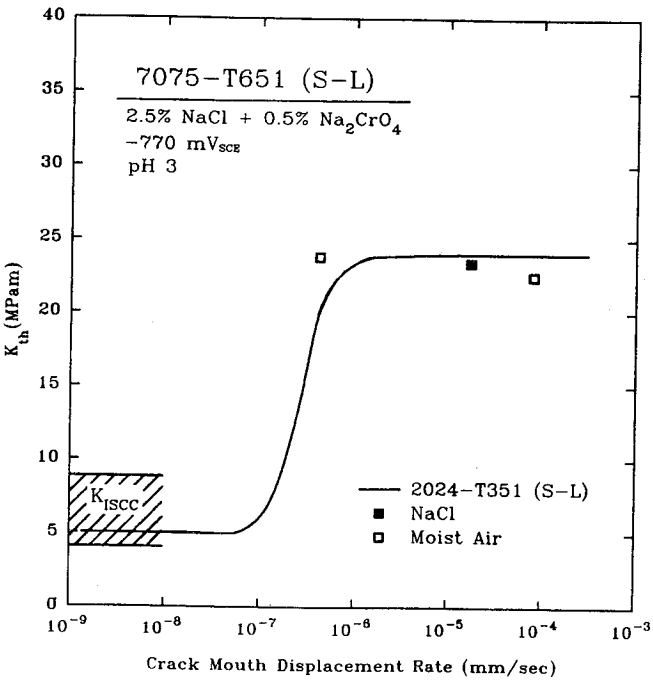

Figure 7 - K_{th} *vs* CMOD rate showing no decrease in K_{th} for increased CMOD rate for the 7075-T651/NaCl system.[19]

Da/dt, measured during the rising load NaCl experiment represented in Fig. 7, equalled 2 to 6 x 10^{-9} m/sec. Similar-rate rising load experiments in moist air produced an apparent da/dt of 1 to 2 x 10^{-9} m/sec at higher K. This result is probably due to temperature and plasticity enhanced resistivity and not subcritical crack growth. Accordingly, da/dt from the NaCl rising load experiment is essentially equal to the quasi-static load da/dt_{SCC} values presented in Fig. 5.[3] Rechberger reported that da/dt varied by 3-fold compared to da/dt_{SCC} as dK/dt increased from 10^{-6} to 10^{-4} MPa√m/sec; however, the precise dependence of da/dt on dK/dt was complex.[11] (At the highest displacement rate for chloride in Fig. 7, dK/dt equals 9 x 10^{-4} MPa√m/sec.) There is no evidence that the

---

2 The EFCP behavior of 7079 shown in Fig. 1 is modeled similarly by linear superposition;[5] however, the reason for the several order of magnitude increase in da/dt_{SCC} is not known.[26]

3 Considering the displacement rate of 2 x 10^{-5} mm/sec, K_{IC} is achieved in 6.5 hours. If da/dt were enhanced by 5 to 10 times above da/dt_{SCC}, sufficient to predict da/dN in Fig. 6, then between 0.4 and 0.8 mm of environmental crack growth would be produced. The complex effects of temperature and plasticity on DCPD measurements are small compared to these crack growth increments, and enhanced da/dt should be measurable.

rising load method provides crack tip strain rate-dependent da/dt values that improve superposition predictions of EFCP kinetics.

A strain rate calculation based on McMeeking's crack tip strain field indicates that the transition CMOD rate in Fig. 7 produces a $d\epsilon_{CT}/dt$ value of 3×10^{-6} sec^{-1} at a distance of one blunted crack tip opening ahead of the tip and at a K level of 8 MPa$\sqrt{m}$ achieved by loading over 100 hours.[30] If the crack surface passive film failure strain is on the order of 1%,[18] then a film rupture event should occur every 3000 seconds at this strain rate and every 15 seconds at the fastest CMOD rate shown in Fig. 7. Since a clean aluminum surface is likely to fully repassivate in less than 10 seconds, the fastest displacement rate is required to begin to electrochemically destabilize the crack tip surface by repeated rupture before full repassivation. Similar lowered electrochemical activity is expected at all CMOD rates below about 10^{-4} mm/sec, equivalent to the quasi-static conditions. If repassivation is more rapid, then even faster strain rates are required to alter da/dt_{SCC}. Environmental cracking did not occur at displacement rates above about 2×10^{-5} mm/sec (and perhaps 10^{-7} mm/sec) because some other step in the damage sequence was presumably rate limiting, and unstable fracture dominated.[31]

Ripple Load Testing

The superposition of a small amplitude cyclic stress intensity, on a constant or slowly rising K, could destabilize mechanically the crack tip surface to enhance electrochemical activity and hence increase da/dt above da/dt_{SCC}. While Bayles and coworkers reported that 7075-T651 is susceptible to enhanced chloride cracking under high frequency, low ΔK "ripple" loading, the stress intensity amplitude employed was sufficiently large to produce process zone volume fatigue damage.[32]

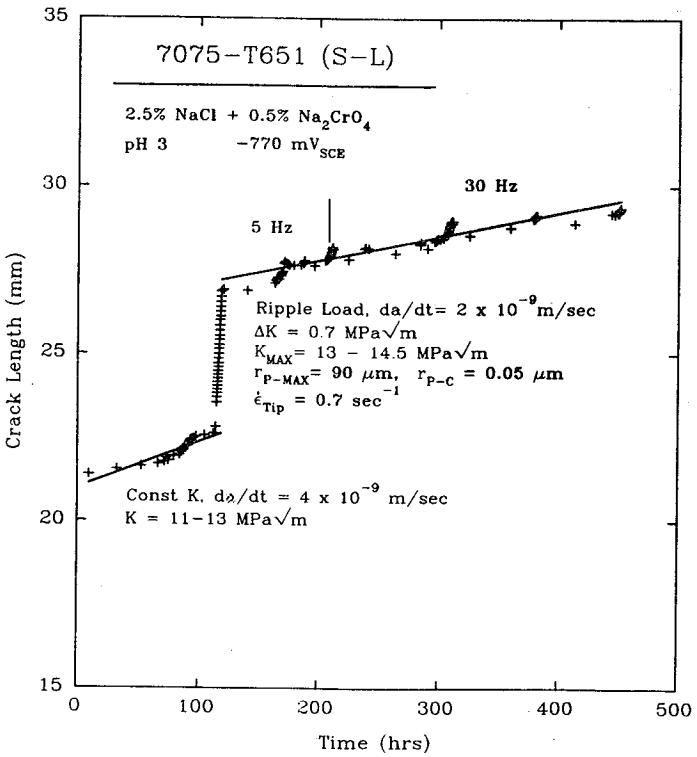

Figure 8 - Crack length vs time showing the results of a constant K (11 to 13 MPa$\sqrt{m}$) with and without applied ripple loading (ΔK = 0.7 MPa$\sqrt{m}$)

In an effort to separate the hypothesized surface-strain enhanced SCC from near-threshold corrosion fatigue, experiments were conducted with a very low amplitude cyclic load, with ΔK equalling 0.7 MPa$\sqrt{m}$, at a frequency of first 5 then 30 Hz. The data plotted in Fig 8 show a negligible difference between the constant stress intensity case and the addition of the low ΔK. For each case, da/dt equalled between 2 and 4 x 10^{-9} m/sec. (The high rate cracking between the constant K and ripple load segments was produced by EFCP at a K_{MAX} of 13 MPa$\sqrt{m}$ and a high ΔK of 11 MPa$\sqrt{m}$.)

The average crack tip near-surface strain rate produced by the ripple load is presumed to be orders of magnitude higher than that for the constant load condition. This conclusion is based on a calculation that equates average $d\epsilon_{CT}/dt$ to the product of frequency, ΔK raised to the fourth power, and a constant defined from a continuum fracture mechanics strain field.[1,30] Average

$d\epsilon_{CT}/dt$ equals between 0.2 sec^{-1} (5 Hz) and 1.2 sec^{-1} (30 Hz), where the critical distance over which this strain rate is calculated was assumed to equal 20% of the cyclic plastic zone diameter (calculated from $0.026\ (\Delta K/\sigma_{YS})^2$). At these rapid strain rates, the crack tip passive film should rupture every 0.01 seconds, resulting in both enhanced anodic dissolution and cathodic atomic hydrogen production. This strain rate is similar to the values relevant to the lower frequency-higher ΔK EFCP conditions that are the target of linear superposition modeling.

Since the measured da/dt in Fig. 8 did not indicate an effect of the ripple load, it is likely that the continuum estimates of strain rate are low. That is, the very small scale of the crack tip cyclic deformation at ΔK of 0.7 MPa$\sqrt{m}$ precluded homogeneous dislocation plasticity sufficient to destabilize the crack tip surface. Since higher ΔK levels could produce process zone fatigue damage, in addition to surface destabilization, ripple load testing does not provide a simple means of defining da/dt for superposition modeling.

Environmental Fatigue Crack Propagation

Since simple linear superposition does not describe EFCP for an important range of frequencies, even for the SCC-susceptible 7075/NaCl system[20], it is necessary to predict time, ΔK and R effects on da/dN based on chemical and mechanical damage within the crack tip process zone.[1,16,18] An element of this approach is to carefully characterize the time and loading waveform dependencies of EFCP rates, and to compare the results, particularly the variability shown in Fig. 1, to crack tip film rupture and hydrogen embrittlement damage mechanisms.

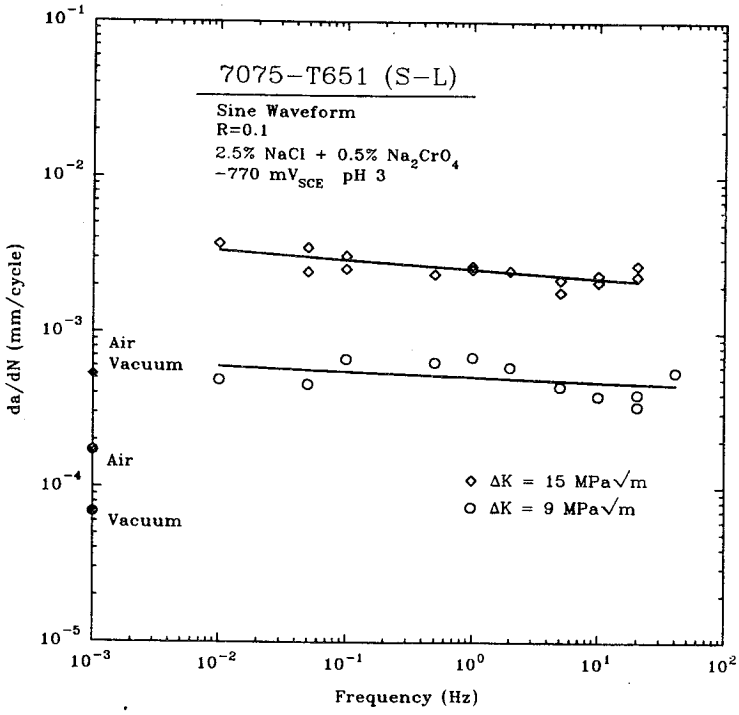

Figure 9 - Da/dN *vs* frequency showing results of constant ΔK (16.8 and 8.5 MPa$\sqrt{m}$) sinusoidal loading for 7075-T651/NaCl.

Effect of Sinusoidal Loading Frequency

Corrosion fatigue crack propagation rates were measured for 7075-T651 (S-L) in NaCl (FI) with sinusoidal loading at frequencies from 20 to 0.01 Hz and a constant R of 0.1. Load was computer-controlled to produce constant ΔK, with the frequency changed after each 2.5 mm of crack growth as monitored by DCPD. A single WOL specimen provided as many as eight constant ΔK segments, as illustrated by the cyclic crack length data in Fig. 3. Da/dN from least squares fits of a vs N data are plotted as a function of frequency in Fig. 9 for high (15 MPa$\sqrt{m}$) and intermediate (9 MPa$\sqrt{m}$) ΔK levels. A parallel Paris law relationship (see Fig. 12) accounted for small (less than 20%) differences in applied ΔK to obtain da/dN for comparison at a single ΔK. FCP rates for this alloy in moist air and vacuum or He[28] are shown to indicate the magnitude of the NaCl effect on da/dN.

EFCP rate decreases mildly with increasing frequency for both ΔK levels, with a very weak frequency dependence ($f^{-0.080}$ for ΔK = 15 MPa$\sqrt{m}$, $f^{-0.074}$ for ΔK = 9 MPa$\sqrt{m}$) observed. This result is consistent with the literature findings for 7075-T6 in Fig. 1, but is in contrast to the $f^{-1/2}$ relationship reported for 7017 and 7475.[6,7]

Effect of Load-Hold-Time

Trapezoidal loading, with varying hold-time at constant K_{MAX}, was employed to define da/dt vs K data that were useful in predicting EFCP rates in high strength steels and nickel-based superalloys.[13] The average time-based crack growth rate was calculated from the difference in measured da/dN at two τ_H values that differed by 100 times, coupled with linear superposition analysis of this load-time history. The implication is that the crack tip strain rates associated with cyclic loading and unloading enhance da/dt over the quasi-static da/dt_{SCC}. In this same study, 7075-T6 (L-T) in chloride exhibited no measurable enhancement of da/dN for hold-times of 0.1 sec and 10 sec.[13]

For 7075-T6 in the S-L orientation, results from corrosion fatigue experiments at two constant stress intensity ranges indicate no strong hold-time-dependence for the loading and unloading rates and times tested. Measured da/dN (e.g., Fig. 3) are plotted vs hold-time at K_{MAX} in Fig 10. Da/dN is essentially constant for relatively rapid rise/fall (t_{Rise} and t_{Fall} = 0.025 sec) trapezoidal waveforms with hold times of 0.1, 5, and 50 seconds. Although mild corrosion-induced closure may account for the small fall in da/dN with increasing τ_H at the higher ΔK, this is more likely due to experimental error and the limited data. In contrast da/dN increases mildly with increasing τ_H for the lower ΔK case, consistent with the results for EFCP under sinusoidal loading (Fig. 9).

Effect of Load-Rise-Time on EFCP

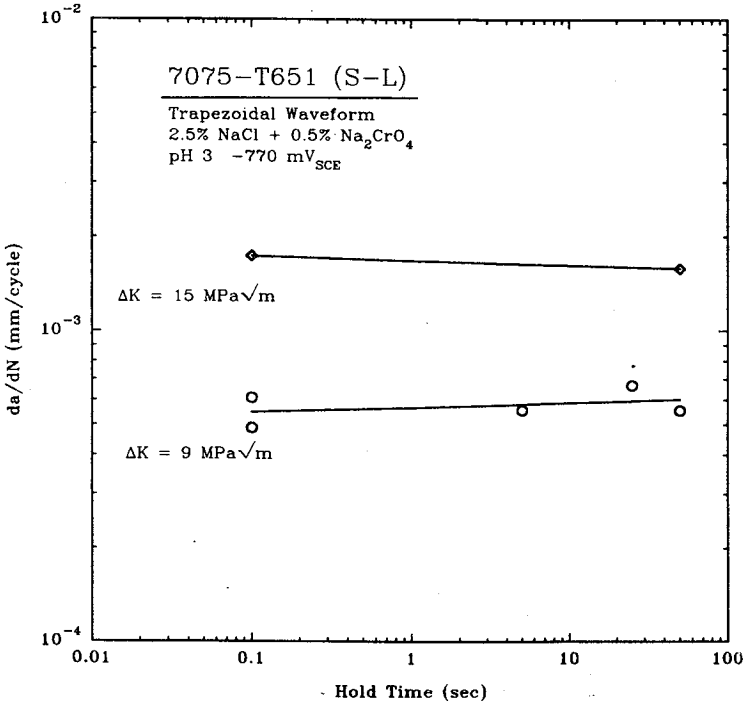

Figure 10 - Da/dN *vs* cycle hold time at K_{MAX} for constant applied ΔK (15, 9 MPa$\sqrt{m}$) for 7075-T651/NaCl, R=0.1.

Constant ΔK and R EFCP experiments were conducted with 7075-T651 (S-L) in NaCl to further examine the effect of loading rise-time (t_R) on da/dN. The results are plotted in Fig. 11 in terms of da/dN vs the rise-time to K_{MAX} for constant ΔK segments including triangular, asymmetric triangular with either a slow/fast or a fast/slow rise/fall sequence, trapezoidal (Fig. 10) and sinusoidal (Fig. 9) K(t) loading functions. Small differences in applied ΔK were accounted for by the wide-range EFCP rate relationship (see Fig. 12). Least squares analyses of these data show that da/dN is proportional to t_R^{λ}, where λ is 0.074 ($\pm$0.018) for ΔK of 9 MPa$\sqrt{m}$ and 0.080 ($\pm$0.021) for ΔK of 15 MPa$\sqrt{m}$.

Since the time-dependence in Fig. 11 is weak, the constant ΔK method is well-suited to resolve the effect of increasing load rise-time. For example, the data in Fig 3 show a vs N for constant ΔK segments and two specimens. Rise-

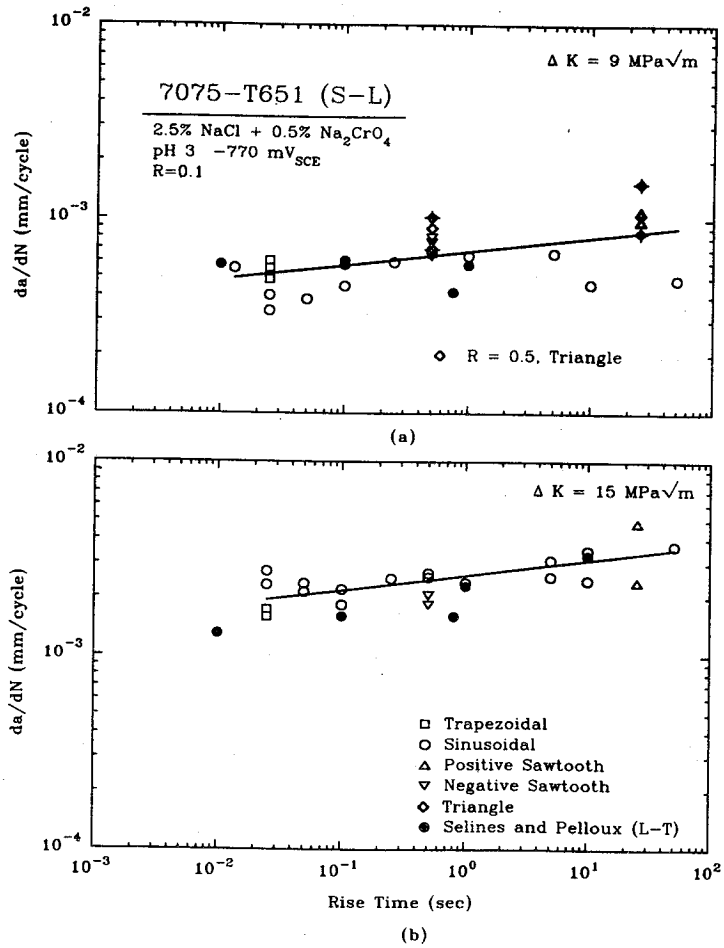

Figure 11 - EFCP da/dN *vs* rise time for 7075-T651: (a) ΔK=9 MPa√m. and (b) ΔK=15 MPa√m. L-T 7075-T6 data are from Selines and Pelloux.[9]

time is varied in the slow/fast to fast/slow sequence, while maintaining total cycle period (see + to ○), and a decrease is noted in the crack growth rate. The results in Fig. 11 are in excellent agreement with data (●) for peak-aged 7075 (L-T) orientation; da/dN is proportional to t_R raised to the 0.10 power.[9] Ouchi et al. showed a similar dependence of da/dN on t_R, with λ equalling 0.3 for a moderate tensile strength alloy steel in NaCl.[33]

Fatigue Crack Closure

The role of fatigue crack closure, specific to corrosion debris produced in the chromate inhibited chloride environment, was investigated by conducting a constant ΔK triangle waveform experiment at a load ratio of 0.5. The resulting EFCP rates are plotted (⟡) in Fig. 11. Da/dN is increased at each rise-time by 30% in response to the increase in R from 0.1 to 0.5. Calculations using a Forman relation, fit to the moist air da/dN vs ΔK data in Fig. 12 to account for plasticity induced closure, predict a 200% increase in da/dN from R of 0.1 to 0.5 at ΔK of 9 MPa√m.[4] If the lesser 30% increase in da/dN is indicative of crack closure, it is not likely due to corrosion debris. Since a substantial amount of plasticity induced closure is predicted, the result in Fig. 11 can not be interpreted based on an intrinsic effect of stress ratio on EFCP. The R of 0.5 results show the same rise time-dependence as the findings for the lower stress ratio. In all cases examined at the lower R, da/dN values were essentially equal when determined at constant ΔK, but at varying crack length and hence total solution exposure time during the experimental sequence (e.g., Fig. 3). 7075-T6 in uninhibited 3.5 wt pct NaCl solution does not show strong corrosion product induced closure effects.[11] Scaling da/dN data obtained at R=0.3[11] to R=0.1, using a Forman relation fit to chloride data to account for plasticity-induced crack closure, yields growth rates that are equal to the current values for inhibited acidified chloride. For this case, the Forman-predicted increase in da/dN at R of 0.3 is less than 200% because the lower slope of the chloride data compared to that for moist air produces a weaker dependency of da/dN on the crack closure function (f) and R. There is no evidence to suggest that the time-dependencies shown in Figs. 9 through 11 are influenced by time-dependent crack closure.

4 Forman equation fit constants: C = 5.148 x 10^{-19}, n = 5.773, P = -21.56, Q = -0.2167.

Summary

The results of all EFCP experiments with S-L 7075-T651 in aqueous chloride are summarized in Fig. 12, compared to the results of the continuous ΔK-decreasing experiment with this alloy in moist air and peak aged 7075 in inert environments.[28] Constant stress ratio ΔK-decreasing NaCl results at 5 Hz (Fig. 6) are represented by the smaller solid diamonds (♦) in Fig 12 and are described by a Paris power-law relation with an exponent of 2.4, as shown by the solid line. The large symbols (♦) for sinusoidal loading represent results from constant ΔK, variable frequency experiments (Fig. 9). The 5 Hz ΔK-decreasing results are in good agreement with the data from the various constant ΔK experiments with sinusoidal loading, as well as with the data for trapezoidal (Fig. 9) and triangular (Fig. 10) K(t) functions.

DISCUSSION

Implications for Life Prediction Modeling

The experimental results for 7075-T651 (S-L) in aqueous NaCl illustrate the complexities of describing EFCP in a fatigue life prediction code such as NASA FLAGRO. While K_{ISCC} is low, da/dt_{SCC} is slow and the simple linear superposition of this quasi-static cracking rate with da/dN_{Mech} only describes frequency, ΔK, waveform and R-value effects on da/dN for slow loading frequencies below about 0.001 Hz and rise times above 500 seconds. Strong environmental effects on da/dN are none-the-less observed for higher frequencies, as illustrated by the data in Fig. 12. From an engineering perspective, EFCP rates in this regime are frequency, waveform and rise-time independent and are well described by the upper bound da/dN-ΔK relationship shown in Fig. 12. This bound, plus linear superposition (Fig. 6) for slow loading cycle periods could be incorporated in FLAGRO to describe the EFCP enhancement.

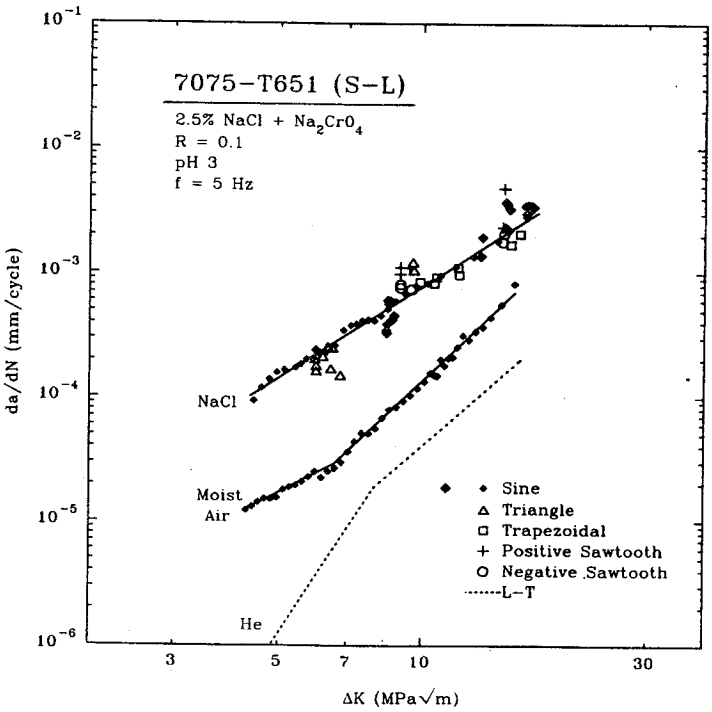

Figure 12 - EFCP data for 7075-T651/NaCl under several loading frequencies, waveforms, and ΔK control formats.

Various loading methods, aimed at increasing the crack tip strain rate above the static load/displacement value, and thus increasing da/dt above da/dt_{SCC} were unsuccessful. This approach does not provide improved superposition predictions of da/dN.

Comparisons between literature data and the new results in Figs. 9 through 12 show that crack orientation has no resolvable effect on EFCP in 7075-T651 for the frequency regime above 0.001 Hz. This is in contrast to the well-known effect of crack orientation on $da/dt_{SCC}(K)$.[17,26] Specifically, the S-L results in Fig. 9 are identical to limited da/dN values

C-6

reported for 7075-T651 in the L-T orientation.[9,13] EFCP rates for trapezoidal loading of the S-L orientation (Fig. 10) are similar to literature data on trapezoidal loading of L-T 7075-T6.[13] The environmental effect on fatigue crack growth is identical for the S-L and T-L orientations with asymmetric triangular loading (Fig. 11).[9] The S-T and T-L orientations of peak aged 7075 exhibit identical FCP rates at a higher stress ratio (R=0.5) for both inert nitrogen and aggressive chloride environments.[34] Since these corrosion fatigue crack growth rates are orientation-independent, it is reasonable to conclude that mildly time-cycle-(in)dependent EFCP does not occur along high angle grain boundaries which are arrayed anisotropically in 7000 series aluminum alloy microstructures. Rather, EFCP may involve more isotropic intersubgranular or brittle transgranular damage processes.

The variability in the time-dependence of da/dN shown in Fig. 1 presents an additional problem to fatigue life prediction because the factors that govern the difference in the behavior of the similar 7000 series alloys are not understood.

Implications for Mechanism-Modeling

Effect of Rising Load and Hold Time on EFCP Rate

To improve linear superposition, Wei and Gao proposed that EFCP rate is composed of three terms according to:[35]

$$\frac{da}{dN} = \frac{da}{dN_{Mech}} + \frac{da}{dN_{CF}} + \int_{\tau} \left[\frac{da}{dt_{SCC}}(K)\right] K(t)\,dt \qquad (3)$$

The first and third terms are analogous to the elements of linear superposition (Eq. 1), while da/dN_{CF} is the rate of time-cycle-dependent EFCP that reflects the synergism between cyclic deformation and chemical reaction. Da/dN_{Mech} and da/dN_{CF} are assumed to proceed in parallel (concurrently), with each occupying a fraction of the crack surface by an identifiable damage process, and can be more precisely stated in terms of such fractional areas.[35] Da/dN_{SCC} occurs in series (consecutively) by an intergranular process for 7000 aluminum alloys. The contribution of da/dN_{SCC} to the sum of the first two terms must be first defined, then the time-cycle-dependence of da/dN_{CF} must be considered based on mass transport and reaction kinetics.[16]

The time dependencies shown in Figs. 9 through 11 (mildly increasing da/dN with decreasing f and increasing t_{Rise}) are not explained sufficiently by superposition of da/dN_{SCC} upon time-independent environment-enhanced da/dN_{CF}. Consider the case of sinusoidal loading represented in Fig. 9 and amplified in Fig. 13. The rising portion of a 0.005 Hz load cycle should produce 1.5×10^{-4} mm of quasi-static load environmental crack advance for ΔK of 15 MPa$\sqrt{m}$ and 2×10^{-4} mm for ΔK of 15 MPa$\sqrt{m}$.[5] For the low ΔK case, da/dN equals 4.2×10^{-4} mm/cycle at 100 Hz and 6.2×10^{-4} mm/cycle at 0.005 Hz, from the trend line. Da/dN_{SCC} accounts for 75% of this EFCP rate increase. For the high ΔK, da/dN increases from 20 to 35×10^{-4} mm/cycle for this same f-range. Da/dN_{SCC} of 2×10^{-4} mm/cycle is clearly small compared to this difference. An identical conclusion is established

5 This calculation assumes that $da/dt_{SCC} = 3 \times 10^{-9}$ m/sec and K_{ISCC} = 5 MPa$\sqrt{m}$, Fig. 5.

by this analysis applied to the rise-time dependencies shown in Fig. 11. (Increasing t_R from 10^{-2} to 10^2 seconds results in da/dN increases from 5 to 9.5 x 10^{-4}mm/cycle and from 20 to 30 x 10^{-4} mm/cycle for the ΔK levels in Fig. 11.)

Interpretation of the hold-time results in Fig. 10 is complicated by limited data and experimental variability. The observed mild decrease in da/dN with increasing τ_H at the higher ΔK is consistent with the nil effect of da/dN_{SCC}. At lower ΔK, da/dN increases from 5.3 to 6.0 x 10^{-4} mm/cycle with increasing τ_H from 0.1 to 50 seconds. This difference is smaller than the predicted contribution from da/dN_{SCC} (1.5 x 10^{-4} mm/cycle). Additional experiments are required to examine the hypothesis that is suggested by these results; da/dN_{CF} is time-independent for fast-rise trapezoidal loading, and is only governed by rise time and the associated active loading rate.

The linear superposition argument also suffers from the presumption that there is some portion of intergranular SCC operating in series with EFCP. This has not been documented here or elsewhere. If the fatigue crack grows along an isotropic intersubgranular or transgranular path, then it is difficult to envision how the crack tip could involve the series operation of a high angle grain boundary path that is tens-of-microns removed from the transgranular tip. The more likely interpretation is that da/dN_{CF} is mildly frequency and rise-time dependent for 7075 in NaCl (FI) for the portion of the time-dependence in Fig. 13 where da/dN is not proportional to reciprocal f. This dependence may be understood based on the kinetics of mass transport and electrochemical reaction.[16]

Variability in Time-Cycle-Dependent Corrosion Fatigue of 7000 Series Aluminum Alloys

Considering time-cycle-dependent EFCP in the three 7000 series alloys represented in Fig. 13, the mild frequency dependence for 7075 is an upper bound on more strongly f-dependent growth in 7017 and 7475. This behavior is amplified in Fig. 14, a plot of the trend line from Fig. 12 with literature data for peak aged 7017 (S-L)[6]. Comparison with EFCP results for 7475 in chloride at 0.1 Hz (the lowest f reported for 7475/NaCl) gives an identical result.[7] The behavior shown in Figs. 13 and 14 can be rationalized based on a critical EFCP rate (da/dN_{Crit}), above which growth is mass transport or reaction rate limited at a specific frequency and compared to single slope power-law behavior at lower rates (and lower ΔK). This transition is shifted to higher da/dN_{Crit} values with decreasing loading frequency and increasing exposure time. EFCP is f-independent, with da/dN equalling da/dN_{Crit}, for all frequencies below the critical value (f_{Crit})

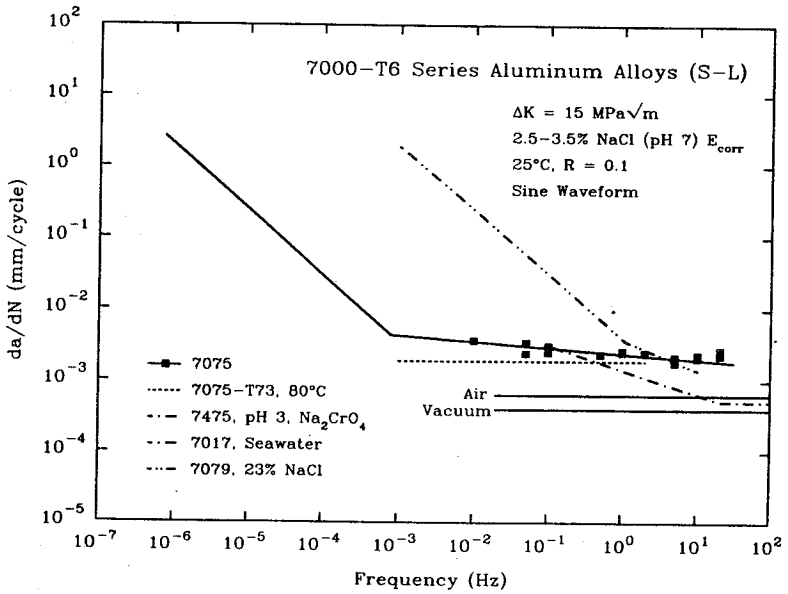

Figure 13 - Comparison of EFCP da/dN *vs* frequency at a constant ΔK (15 MPa√m) for the S-L orientation of several 7000 series aluminum alloys with results for 7075-T651.

corresponding to da/dN_{Crit}.[6] EFCP is f-dependent for faster frequencies. This interpretation is supported by fractographic observations that demonstrate a transition from brittle transgranular cracking to ductile-striated cracking, with increasing da/dN through the transition level, for both 7017 and 7475.[6,7]

The behavior of 7075 compared to 7475 and 7017 is understood if it can be shown that da/dN_{Crit} is higher for the former alloy, at a given frequency, or that f_{Crit} for a given da/dN_{Crit} is higher relative to the fastest frequencies examined for 7075 in the current and previous studies.[5,11] At the single ΔK level and frequencies represented in Fig. 13, 7075 is cracking in the "*below* da/dN_{Crit} - f_{Crit}" regime, while 7017 and 7475 are in the "*above* da/dN_{Crit} - f_{Crit}" regime. At faster frequencies, da/dN would be time-cycle-dependent for 7075. The former case involves essentially time-cycle-independent cracking ($da/dN \propto f^0$ to $f^{-0.1}$), while the latter obeys a stronger time-dependence ($da/dN \propto f^{-0.5}$). It is difficult to develop this hypothesis because the environmental cracking mechanism is controversial, be it hydrogen environment embrittlement, film rupture/transient repassivation, or a coupling of each. Additionally, the transport plus reaction sequence that feeds these mechanisms is multi-featured.[1,16]

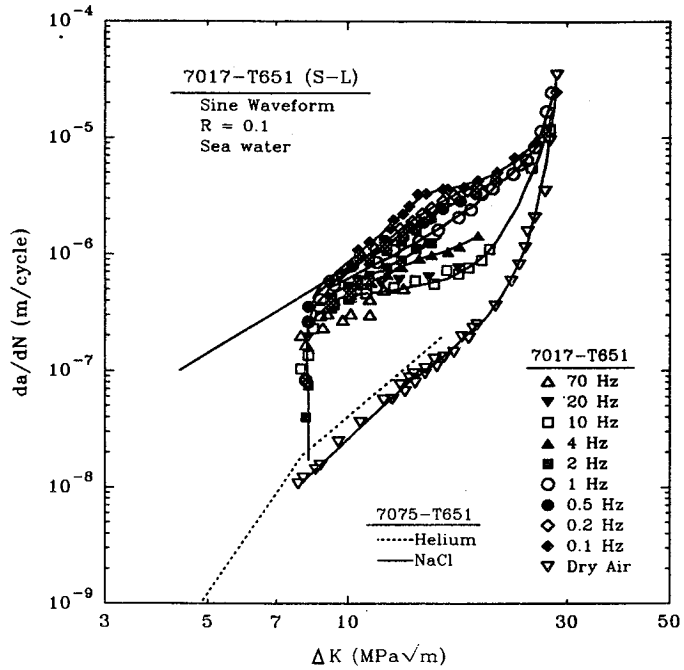

Figure 14 - Effect of ΔK on da/dN for peak aged 7075 and 7017[6] in chloride showing upper bound, f-independent EFCP.

To illustrate a speculative explanation for the time-cycle-dependencies in Fig. 13, consider that EFCP in 7000 series aluminum alloys is due to crack tip hydrogen environment embrittlement.[1] Da/dN_{Crit} is rate limited by hydrogen diffusion in the highly strained crack tip process zone.[6,7] This scenario requires that crack solution mass transport and crack surface reactions are comparatively rapid, as is reasonable for the strain-disrupted crack tip in an aluminum alloy in chloride. Assume that da/dN equals the extent of crack advance (Δx) per a number of load cycles ($N = f\Delta t$, where Δt is the time expired to produce N) which may be 1 or larger. Δx is governed by the ΔK-based mechanics of process zone fatigue damage. Da/dN_{Crit} then corresponds to the growth rate at which hydrogen diffusion is just sufficient to penetrate to a critical concentration, over Δx in Δt. This relationship was formalized to predict the frequency dependence of da/dN_{Crit}:[6,7]

$$\frac{da}{dN_{crit}} = \frac{2}{\sqrt{f\,N}} \sqrt{D_H}\; erf^{-1}\left(1 - \frac{C_{Crit}}{C_S}\right) \qquad (4)$$

D_H is the diffusivity of hydrogen in aluminum, be it grain boundary, lattice or dislocation transport.

---

6 Below f_{Crit} and da/dN_{Crit}, the results in Figs. 9 through 11 and 13 demonstrate that da/dN is mildly time-cycle-dependent.

C_{Crit} is the amount of hydrogen that must be provided for cracking at the deepest point of the fatigue damage distribution within the process zone, and C_S is the concentration of the atomic hydrogen on the crack tip surface in equilibrium with the occluded crack tip solution electrochemistry. This equation predicts that da/dN_{Crit} varies as $f^{-0.5}$, as would all da/dN-ΔK values above this level if simple parallel slope behavior is operative, as illustrated schematically in Fig. 15.

Green and Knott compared Eq. 4 to EFCP rates for 7475 in acidified and inhibited NaCl.[7] Da/dN_{Crit} varied with $f^{-0.5}$; these data yielded D_H of 5 x 10^{-9} cm^2/sec and C_{Crit}/C_S of 0.14, assuming per-cycle crack advance. A similar result was reported by Holroyd and Hardie for 7017 in seawater with an inferred D_H of 3 x 10^{-9} cm^2/sec and C_{Crit}/C_S of 0.3.[6] These diffusivities are an order of magnitude faster than lattice D_H for aluminum alloys, suggesting that grain boundary or subgrain/ dislocation pipeline hydrogen diffusion is important even for transgranular EFCP in these alloys.

Considering the alloy-dependence of da/dN_{Crit}, higher values of this rate at fixed f are favored by increased D_H and C_S, and by decreased C_{Crit} and N (Eq. 4). Speculatively, dislocation transport could increase D_H to a value as high as 5 x 10^{-7} cm^2/sec;[36] da/dN_{Crit} would be raised by 10-fold, or the bounding f required for rate-limited EFCP would be increased by two orders of magnitude. Frequencies on the order of 200 Hz would be required for time-cycle-dependent da/dN at moderate ΔK levels. There is no reason to implicate dislocation transport in 7075, but not in 7475 or 7017, and the notion of dislocation transport of H in aluminum alloys has been challenged.[37] Dislocation transport may be by enhanced pipe diffusion of hydrogen through the crack tip dislocation structure produced by cyclic plastic deformation. This structure could be deformation mode and alloy-dependent.

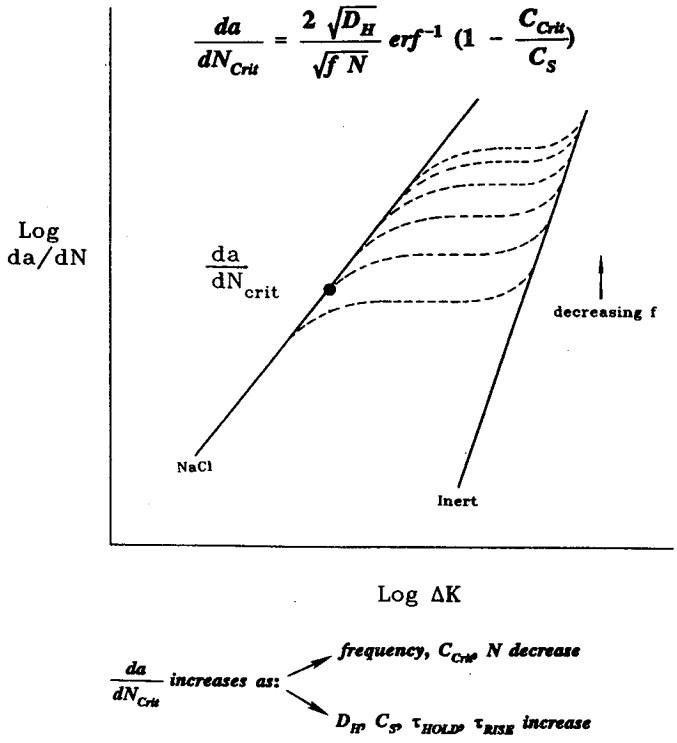

Figure 15 - Schematic EFCP da/dN vs ΔK showing the f dependence of da/dN and da/dN_{crit}.

Alternately, C_S could be alloy-dependent. For example, Zn or Mg could be present in varying amounts in precipitates, lattice solid solution, or segregated to grain boundaries. These elements could preferentially dissolve to enrich the crack solution in cations which in turn could increase C_S by affecting the ratio between the absorption and desorption rate constants involved in H production on the crack surface.[7] A surface film enriched in a segregant could also affect such a change. Mg segregation to grain boundaries in 7000 series aluminum alloys has been documented.[38-40] Cation effects on electrochemistry, and surface film effects on H entry, have not been substantiated by either crack chemistry measurements or permeation experiments with aluminum alloys. Alternately, Anyalebechi demonstrated that C_S in aluminum is enhanced by solid solution elements such as Li;[41]

7 J. R. Scully, personal communication (1994).

the role of Mg in this regard is unclear. C_{Crit} depends on the structure and local strength of the sites of hydrogen-enhanced fatigue damage. It is unknown how this concentration varies with alloy microstructure and cyclic deformation processes.

Similar arguments for the variability in the frequency dependence of EFCP rates in 7000 series aluminum alloys could be suggested based on alloy effects on surface reaction kinetics,[16,38,42] particularly if the crack tip surface is filmed and competitively bared by strain. Explanations based on crack solution mass transport control are not apparent because of uncertainties in the molecules and ions that rate limit surface reactions. The problem is complex and any explanation is speculative. Measurements of crack chemistry, hydrogen production and passivation kinetics are required to define the composition and microstructural features of 7000 series alloys that determine whether EFCP rate is time-independent, time-cycle dependent, or time-dependent.

CONCLUSIONS

1. Fatigue crack propagation rates for 7075-T651 (S-L orientation) in chromate inhibited, acidified NaCl solution are enhanced five to ten-fold over rates in moist air and are over an order of magnitude faster compared to cracking in helium.

2. Measured time-based crack growth rates for 7075-T651 (S-L), subjected to quasi-static load or displacement, are an order of magnitude too small to predict the effect of NaCl on FCP rates for loading frequencies above 0.001 Hz and by linear superposition.

3. Alternate methods of establishing da/dt, based on enhanced crack tip strain rate, do not provide a means of enabling linear superposition modeling of EFCP in peak-aged 7075/NaCl. Imposed constant crack mouth opening displacement rate does not accelerate da/dt. Da/dt is not enhanced by high frequency-low amplitude cyclic loading, designed to increase crack tip surface strain rate, in conjunction with a high sustained stress intensity.

4. Crack propagation rates for corrosion fatigue of 7075-T651 (S-L) in NaCl show two regimes of frequency dependence; da/dN is proportional to f^{-1} below 0.001 Hz and proportional to $f^{-\lambda}$, where λ is between 0 and 0.1, for f above 0.001 Hz. Da/dN and da/dN_{CF} increase mildly with increasing rise-time for a range of loading waveforms but may not depend on hold-time at K_{MAX}. The strong frequency dependence is modeled based on simple linear superposition, while the mild time-dependence is due to cycle-time-dependent corrosion fatigue.

5. The NaCl environmental effect on time-cycle-dependent fatigue crack growth is identical for the S-L and L-T orientations of peak aged 7075, suggesting a minimal involvement of anisotropic high angle grain boundaries.

6. The frequency response of EFCP in 7000 series alloys is variable and depends on an undefined compositional or microstructural variable. Crack solution cations, from segregant or a second phase in the alloy, could alter hydrogen production kinetics, or H diffusion within the crack tip process zone could vary based on dislocation and grain boundary

processes. High hydrogen production/uptake and rapid hydrogen diffusion favor f-independent cracking persisting to higher frequencies and crack growth rates.

7. EFCP in the 7075/NaCl system is adequately described for computer life prediction by linear superposition for long load-cycle periods, and by a time-independent upper bound relationship between da/dN and ΔK for moderate frequencies and load rise-times.

ACKNOWLEDGEMENTS

This research was supported by the Mechanics of Materials Branch at the NASA Langley Research Center, under Grant No. NAG-745-1, with R.S. Piascik and J.C. Newman, Jr. as technical monitors. AA7075 was provided by E.A. Colvin of the Alcoa Technical Center. E. Richey contributed experimental results. This support is gratefully acknowledged. The need to incorporate environmental effects into NASA FLAGRO was suggested by R.G. Forman at the NASA-Johnson Space Flight Center.

REFERENCES

1. Gangloff, R. P.: Corrosion Fatigue Crack Propagation in Metals. in *Environment-Induced Cracking of Metals Proceedings*, Gangloff, R. P. and Ives, M. B., eds, NACE, Houston, TX, 1990, pp. 55-109.

2. Feeney, J. A.; McMillan, J. C.; and Wei, R. P.: Environmental Fatigue Crack Propagation of Aluminum Alloys at Low Stress Intensity Levels. *Metall. Trans. A*, vol. 1, 1970, pp. 1741-1757.

3. Forman, R. G.; Shivakumar, V.; Newman, J. C.; and Piotrowski, S. M.; and Williams, L. C.: Development of the NASA/FLAGRO Computer Program in *Fracture Mechanics: 18th Symposium, ASTM STP 945*, ASTM, Philadelphia, PA, 1988, pp. 781-803.

4. Gangloff, R. P.; Piascik, R. S.; Dicus, D. L.; and Newman, J. C.: Fatigue Crack Propagation in Aerospace Aluminum Alloys. *Journal of Aircraft*, vol. 31, 1994, pp. 720-729.

5. Speidel, M. O.: Stress Corrosion and Corrosion Fatigue Crack Growth in Aluminum Alloys. in *Stress Corrosion Research*, Arup, H.; and Parkins, R. N., eds., Sijthoff & Noordhoff, Alphen aan den Rijn, Netherlands, 1979, pp. 117-176.

6. Holroyd, N. J. H.; and Hardie, D.: Factors Controlling Crack Velocity in 7000 Series Aluminum Alloys During Fatigue in an Aggressive Environment. *Corrosion Science*, vol. 23, 1983, pp. 527-546.

7. Green, A. M.; and Knott, J. F.: Effects of Environment and Frequency on the Long Fatigue Crack Growth of Aluminum Alloy 7475. in *Advances in Fracture Research*, Salama, K.; Ravi-Chandar, K.; Taplin, D. M. R.; and Rao, R. P., eds., Pergamon Press, Oxford, UK, 1989, pp. 1747-1756.

8. Baldantoni, A.; Wallace, W.; Raizenne, M. D.; and Dickson, J. Y.: The NRC Contribution to the FACT Programme. in *The Fatigue in Aircraft Corrosion Testing (FACT) Programme*, Wanhill, R. J. H.; De Luccia, J. J.; and Russo, M. T., eds., AGARD Report No. 713, NATO, 1985, pp. 162-173.

9. Selines, R. J.; and Pelloux, R. M.: Effect of Cyclic Stress Wave Form on Corrosion Fatigue Crack Propagation in Al-Zn-Mg Alloys. *Metall. Trans. A*, vol. 3, 1972, pp. 2525-2531.

10. Kim, Y. H.; and Manning, S. D.: A Superposition Model for Corrosion-Fatigue Crack Propagation in Aluminum Alloys. in *Fracture Mechanics: Fourteenth Symposium - Volume 1: Theory and Analysis, ASTM STP 791*, Lewis, J. C.; and Sines, G., eds., American Society for Testing and Materials, Philadelphia, PA, 1983, pp. 446-462.

11. Rechberger, J.: *The Transition from Stress Corrosion Cracking to Corrosion Fatigue in AA-7075 and AA-8090.* Ph.D. Dissertation, University of British Columbia, Vancouver, Canada, 1989.

12. Barsom, J. M.: Effect of Cyclic Stress Form on Corrosion Fatigue Crack Propagation Below K_{ISCC} In a High Yield Strength Steel. in *Corrosion Fatigue, Chemistry, Mechanics, and Microstructure*, Devereaux, O.; McEvily, A. J.; and Staehle, R. W., eds., NACE, Houston, TX, 1972, pp. 424-436.

13. Dill, H. D.; and Saff, C. R.: *Environment-Load Interaction Effects on Crack Growth.* AFFDL-TR-78-137, McDonnell Douglas Corp., St. Louis, MO, 1978.

14. Larsen, J. M.; and Nicholas, Theodore: Cumulative Damage Modeling of Fatigue Crack Growth. in *AGARD Advisory Group for Aerospace Research and Development, Conference Proceedings No. 368*, NATO, 1987.

15. Wei, R. P.; and Landes, J. D.: Correlation Between Sustained-Load and Fatigue Crack Growth in High-Strength Steels. *Materials Research and Standards*, vol. 9, 1969, pp. 25-27,44-48.

16. Wei, R. P.; and Gangloff, R. P.: Environmentally Assisted Crack Growth in Structural Alloys: Perspectives and New Directions. in *Fracture Mechanics: Perspectives and Directions, ASTM STP 1020*, Wei, R. P.; and Gangloff, R. P., eds., ASTM, Philadelphia, PA, 1989, pp. 233-264.

17. Speidel, M. O.: Stress Corrosion Cracking of Aluminum Alloys. *Metall. Trans. A*, vol. 6A, 1975, pp. 631-651.

18. Ford, F. P.: The Crack-Tip System and Its Relevance to the Prediction of Cracking in Aqueous Environments. in *Environment-Induced Cracking of Metals*, Gangloff, R. P.; and Ives, M. B., eds., NACE, Houston, TX, 1988, pp. 139-165.

19. Dietzel, W.; Schwalbe, K. H.; and Wu, D.: Application of Fracture Mechanics Techniques to the Environmentally Assisted Cracking of Aluminum 2024. in *Fatigue and Fracture of Engineering Materials and Structures*, vol. 12, 1989, pp. 495-510.

20. Colvin, E. L.; and Emptage, M. R. (1991), The Breaking Load Method. in *New Methods for Corrosion Testing of Aluminum Alloys, ASTM STP 1134*, Agarwala, V. S.; and Ugiansky, G. M., eds., ASTM, Philadelphia, PA, 1992, pp. 82-100.

21. Saxena, A.; and Hudak, S. J., Jr.: Review and Extension of Compliance Information for Common Crack Growth Specimens. *Int. J. of Frac.*, vol. 14, No. 5, 1978, pp. 453-468.

22. Standard Test Method for Measurement of Fatigue Crack Growth Rates. Designation E647-91 in *1991 Annual Book of ASTM Standards*, ASTM, Philadelphia, PA, pp. 674-701, 1991.

23. Donald, J. K.; and Ruschau, J.: Direct Current Potential Difference Fatigue Crack Measurement Techniques. in *Fatigue Crack Measurement: Techniques and Applications*, Marsh, K. J.; Smith, R. A.; and Ritchie, R. O., eds., EMAS, Ltd., West Midlands, UK, 1991, pp. 11-37.

24. Thompson, J. J.; Tankins, E. S.; and Agarwala, V. S.: A Heat Treatment for Reducing Corrosion and Stress Corrosion Cracking Susceptibilities in 7XXX Aluminum Alloys. *Materials Performance*, vol. 26, No. 6, 1987, pp. 45-52.

25. Le, A. H.; and Foley, R. T.: Stress Corrosion Cracking of 7075-T651 in Various Electrolytes - Statistical Treatment of Data Obtained Using DCB Precracked Specimens. *Corrosion Science*, vol. 39, No. 10, 1983, pp. 379-383.

26. Holroyd, N. J. H.: Environment-Induced Cracking of High-Strength Aluminum Alloys. in *Environment-Induced Cracking of Metals*, Gangloff, R. P.; and Ives, M. B., eds., NACE, Houston, TX, 1988, pp. 311-345.

27. Domack, M. S.: Evaluation of K_{ISCC} and da/dt Measurements for Aluminum Alloys Using Precracked Specimens. in *Environmentally Assisted Cracking: Science and Engineering ASTM STP 1049*, Lisagor, W. B.; Crooker, T. W.; and Leis, B. N., eds., ASTM, Philadelphia, PA, 1990, pp. 391-409.

28. Piascik, R. S.; and Gangloff, R. P.: Environmental Fatigue of an Al-Li-Cu Alloy: Part I. Intrinsic Crack Propagation Kinetics in Hydrogenous Environments. *Metall. Trans. A*, vol. 22A, 1991, pp. 2415-2428.

29. Richey, E., III; Wilson, A. W.; Pope, J. M.; and Gangloff, R. P., *Computer Modeling the Fatigue Crack Growth Rate Behavior of Metals in Corrosive Environments*, University of Virginia Report, Charlottesville, VA, in press, 1994.

30. Young, L. M.: *Environment Assisted Cracking in Beta-Titanium Alloys*. MS Thesis, University of Virginia, Charlottesville, VA, 1993.

31. Holroyd, N. J. H.; and Hardie, D.: Strain-Rate Effects in the Environmentally Assisted Fracture of a Commercial High-Strength Aluminum Alloy (7049). *Corrosion Science*, vol. 21, 1981, pp. 129-144.

32. Bayles, B. A.; Pao, P. S.; Gill, S. J.; and Yoder, G. R.: Ripple-Load Cracking in Three Alloys Systems. in *Systems Engineering Approach to Mechanical Failure Prevention*, Pusey, H. C.; and Pusey, S. C., eds., Vibration Institute, Willowbrook, IL, 1993, pp. 167-176.

33. Ouchi, H.; Kobayashi, J.; and Soya, I.: Formulation of Stress Waveform and Frequency Effects on Fatigue Crack Growth Rates in Steel Immersed in Seawater. Nippon Steel Corporation, Kanagawa, Japan, Unpublished Report, 1988.

34. Santner, J. S.; and Kumar, M.: Corrosion-Fatigue Crack Propagation Rates in Commercial 7075 and P/M X7091 Aluminum Alloys. in *Corrosion Fatigue: Mechanics, Metallurgy, Electrochemistry, and Engineering ASTM STP 801*, Crooker, T. W.; and Leis, B. N., eds., ASTM, Philadelphia, PA, 1983, pp. pp. 229-255.

35. Wei, R. P.; and Gao, M.: Reconsideration of the Superposition Model for Environmentally Assisted Fatigue Crack Growth. *Scripta Metall.*, vol. 17, 1983, pp. 959-962.

36. Albrecht, J.; Bernstein, I. M.; and Thompson, A. W.: Evidence for Dislocation Transport of Hydrogen in Aluminum. *Metall. Trans. A*, vol. 13A, 1982, pp. 811-819.

37. Watson, James W.; and Meshii, M.: Hydrogen Transported by Dislocations in Aluminum Alloys. in *Hydrogen Effects on Material Behavior*, Moody, N. R.; and Thompson, A. W., eds., TMS-AIME, Warrendale, PA, 1990, pp. 241-248.

38. Wei, R. P.; Gao, Ming; and Pao, P. S.: The Role of Magnesium in CF and SCC of 7000 Series Aluminum Alloys. *Scripta Metall.*, vol. 18, 1984, pp. 1195-1198.

39. Holroyd, N. J. H.; and Scamans, G. M.: The Role of Magnesium During Environment-Sensitive Fracture of Aluminum Alloys. *Scripta Metall.*, vol. 19, 1985, pp. 915-916.

40. Shastry, C. R.; Levy, M.; and Joshi, A.: The Effect of Solution Treatment Temperature on Stress Corrosion Susceptibility of 7075 Aluminum Alloy. *Corrosion Science*, vol. 21, 1981, pp. 673-688.

41. Anyalebechi, P. N.; Talbot, D. E. J.; and Granger, D. A.: Hydrogen Solution in Al-Li Alloys. in *Light-Weight Alloys for Aerospace Applications*, Lee, E. W.; Chia, E. H.; and Kim, N. J., eds., TMS-AIME, Warrendale, PA, 1989, pp. 249-270.

42. Gao, M.; Pao, P. S.; and Wei, R. P.: Chemical and Metallurgical Aspects of Environmentally Assisted Fatigue Crack Growth in 7075-T651 Aluminum Alloy. *Metall. Trans. A*, vol. 19A, 1988, pp. 1739-1750.